Conference paper

Majed Chergui*

Empirical rules of molecular photophysics in the light of ultrafast spectroscopy

Abstract: The advent of ultrafast laser spectroscopy has allowed entirely new possibilities for the investigation of the ultrafast photophysics of inorganic metal-based molecular complexes. In this review we show different regimes where non-Kasha behavior shows up. We also demonstrate that while ultrafast intersystem crossing is a common observation in metal complexes, the ISC rates do not scale with the magnitude of the spin-orbit coupling constant. Structural dynamics and density of states play a crucial role in such ultrafast ISC processes, which are not limited to molecules containing heavy atoms.

Keywords: fluorescence spectroscopy; intramolecular relaxation; molecular dynamics; photochemistry; transition metals; UV-visible spectroscopy; XXV IUPAC Photochemistry.

DOI 10.1515/pac-2014-0939

Introduction

The advent of ultrafast spectroscopy some 25 years ago triggered a real revolution in photochemistry and photophysics due to its ability to probe photoinduced processes on the time scale of molecular vibrations [1]. In the study of condensed phase systems (molecules in solution, proteins, materials), an impressive variety of experimental methodologies has been used and developed, such as pump-probe transient absorption spectroscopy in the visible to the infrared spectral ranges [1], fluorescence up-conversion [2, 3], non-linear optical techniques (photon echo, transient grating) [4], and more recently, multidimensional spectroscopies [5–10]. Many of these have been extended to other spectral ranges, such as the UV for non-linear [11–14] and multidimensional spectroscopies [8, 9, 15–19] or the X-ray for transient absorption spectroscopy [20, 21]. All these tools have provided unsurpassed insight into the ultrafast photoinduced chemical dynamics of molecular systems.

The first events upon absorption of a photon by a large molecule is the redistribution of energy among different electronic and vibrational degrees of freedom, which may in some cases, lead to unimolecular reactions such as dissociation, predissociation and isomerization. In addition, intramolecular energy redistribution proceeds via different non-radiative processes, such as internal conversion (IC), i.e. the transition between electronic states of the same spin, intersystem crossing (ISC), which is the transition between states of different spin multiplicities and intramolecular vibration redistribution (IVR), which involves vibrational energy flow from a given vibrational mode (or modes) to others.

Article note: A collection of invited papers based on presentations at the XXVth IUPAC Symposium on Photochemistry, Bordeaux, France, July 13–18, 2014.

***Corresponding author: Majed Chergui,** Ecole Polytechnique Fédérale de Lausanne, Laboratoire de Spectroscopie Ultrarapide, ISIC, Faculté des Sciences de Base, Station 6, CH-1015 Lausanne, Switzerland, e-mail: Majed.chergui@epfl.ch

In the decades preceding the era of ultrafast lasers, a body of work carried out mainly by static or time-resolved emission spectroscopy with resolutions of the nanosecond or more, lead to the emergence of a number of general empirical rules in molecular photophysics [22], of which two of the most important ones are:

1. The Kasha rule, proposed in 1950 [23], and states that photon emission (fluorescence or phosphorescence) occurs in appreciable yield only from the lowest excited state of a given multiplicity. A corollary of Kasha's rule is the Kasha–Vavilov rule, which states that the quantum yield of luminescence is generally independent of the excitation wavelength [24]. This can be understood as a consequence of the tendency – implied by Kasha's rule – for molecules in upper states to relax to the lowest excited state non-radiatively.
2. The heavy atom effect, which is defined by IUPAC as "The enhancement of the rate of a spin-forbidden process (the radiative is called phosphorescence, while non-radiative is called the intersystem crossing) by the presence of an atom of high atomic number, which is either part of, or external to, the excited molecular entity. Mechanistically, it responds to a spin-orbit coupling enhancement produced by a heavy atom" [25].

As already mentioned, these rules were postulated well before the advent of pulsed femtosecond lasers. In particular, the heavy atom effect implies that the state from which the ISC departs is a quasi-stationary one (i.e., it has developed its stationary wave function). In deriving the ISC rate k_{ISC}, the theory is based on the Fermi golden rule and the Born–Oppenheimer approximation:

$$k_{ISC} \propto H_{SO}^2 \langle v_i | v_f \rangle^2 \rho \tag{1}$$

Where H_{SO} is the spin-orbit coupling (SOC) constant, v_i, v_f are the vibrational wave functions of the initial and final electronic states of the ISC transition and ρ is the density of states. The change of spin quantum number that comes about this transition has to be compensated by a rotation of the orbital momentum in order for the total angular momentum to be conserved. This is called first order SOC [26]. When this is not possible, asymmetric vibrations may compensate for the change of spin angular momentum, in which case we speak of second order SOC.

In this short review, we show that the advent of ultrafast spectroscopies calls for a revision of the above empirical rules.

Experimental strategies

The first developed and most commonly used technique in ultrafast spectroscopy is the pump–probe scheme, which is basically an extension to ultrashort times of the traditional flash photolysis technique [27, 28]. In this scheme (Fig. 1) a first (pump) pulse excites the system, triggering a photophysical or photochemical process, and a second (probe) pulse interrogates the evolution of the excited state (or states) by absorption to higher states or by stimulated emission (SE). Both of these signals may overlap each other, and also the transparency of the sample induced by the pump pulse (called ground state bleach, GSB), if the ground state absorption spectrum is in the same spectral range (Fig. 2). With the development of non-linear optics it has become possible not only to reach very short pulse durations in the order of a few femtoseconds, but also and most important, to generate ultrashort continua that could be used to probe the dynamics of molecular systems over an extended wavelength range.

As already mentioned, most studies that led to the development of the above empirical rules were based on the study of the emission spectra of molecules. Following the ultrafast evolution of excited states by emission is ideal because it removes the problem of overlapping signals that occurs in transient absorption spectroscopy (Fig. 2).

The fastest detectors for fluorescence are streak cameras but these reach at best a time resolution of a few picoseconds. To go to shorter times, optical sampling methods such as fluorescence up- or down-conversion

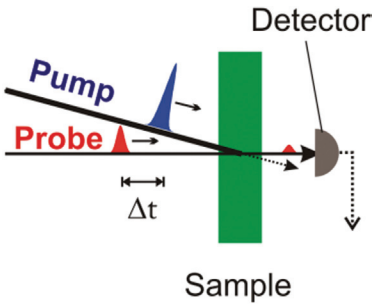

Fig. 1: Principle of the pump-probe experiment: A first laser (pump) pulse excites the sample at time t = 0. A second (probe) laser pulse, whose time delay Δt can be tuned with respect to the pump pulse, records the evolution of the system at a given configuration.

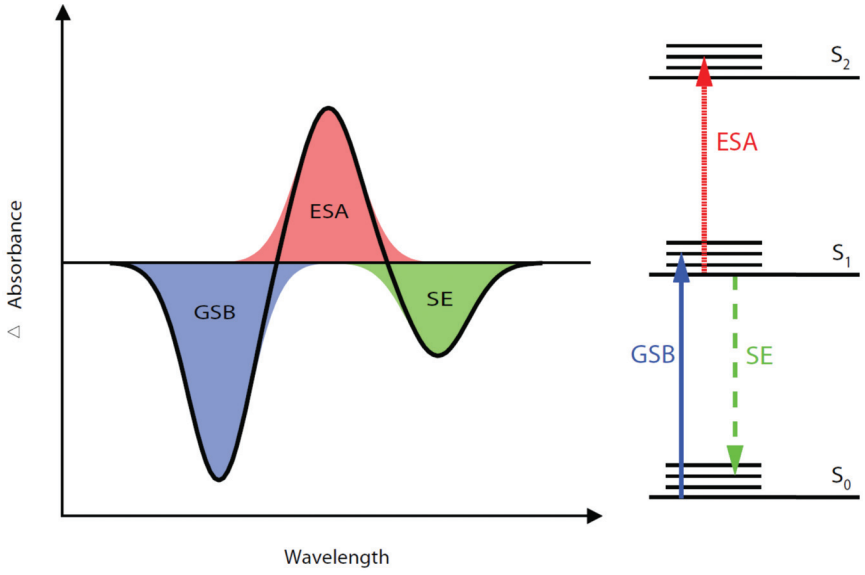

Fig. 2: Possible types of signals obtained in a pump-probe transient absorption experiment. The absorbance (or optical density) of the excited sample minus that of the unexcited is plotted as a function of probe wavelength. Depopulation of the ground state (S0) leads to a decreased absorbance (or increased transparency), which is due to the ground state bleach (GSB). Excited state absorption (ESA) gives rise to an increased absorbance, while stimulated emission (SE) gives rise to a decreased absorbance, just as GSB.

are ideal and have been pushed into the femtosecond regime [29–31], enabling detection of extremely short lived emission signals. Indeed, even for very short lived excited singlet states, there is a non-zero probability of emitting photons, which can be detected if the time window of the detection is adequately narrow. An important improvement to the technique came with the introduction of CCD cameras coupled to a monochromator, allowing a polychromatic detection and therefore, bringing a significant increase in signal-to-noise and speed of data acquisition [32–35]. Figure 3 shows a sheme of our set-up. The fluorescence is collected by wide-angle optics and focused onto a non-linear crystal in which it is mixed with a so-called, gate pulse, whose time delay with respect to the pump pulse is controlled by an optical delay stage. The intensity of the signal resulting from the sum- (or difference-) frequency of the gate pulse with the fluorescence is then recorded as a function of the delay time between pump and gate pulses.

Figure 4 illustrates the capability of our set-up showing how the entire emission spectral profile can be recorded at each time delay. We have extended its detection to the mid-IR [37] and to the UV around 300 nm [33].

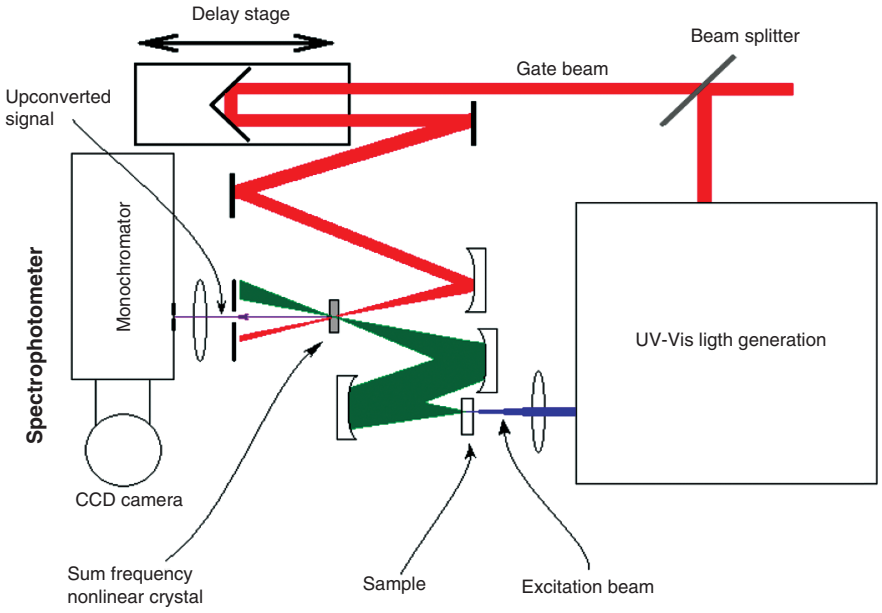

Fig. 3: Set-up for fluorescence up-conversion with broad band detection for the measurement of ultrafast decay times [36]. The green area represents the fluorescence from the sample that is collected by wide angle optics and focussed onto the non-linear crystals where it overlaps the focus of the gate beam.

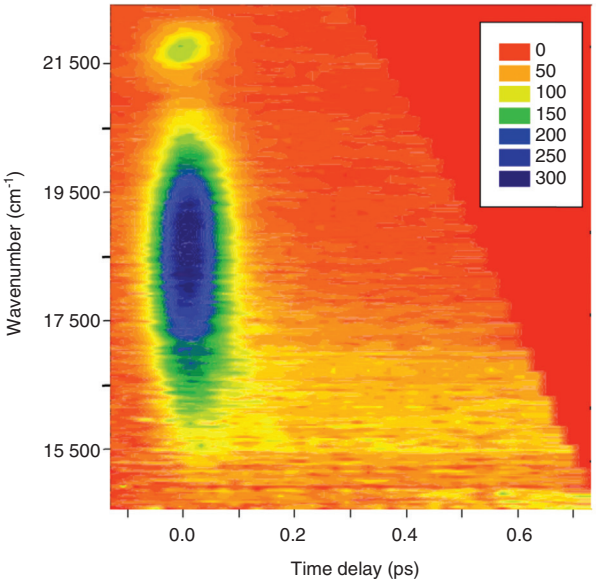

Fig. 4: Emission of $[Ru(bpy)_3]^{2+}$ in water as a function of time upon excitation at 400 nm. The signal around t = 0 between 16 500 (606 nm) and 20 000 cm^{-1} (500 nm) is due to the fluorescence of the singlet metal-to-ligand-charge-transfer (^{1}MLCT) state, while the yellow stripe centered around 16 400 cm^{-1} (609.75 nm) is due to the ^{3}MLCT phosphorescence. The spot at 21 600 cm^{-1} (430 nm) is the Raman band of the solvent [33].

In this short review, we mainly focus on our results from a combination of ultrafast and steady-state emission studies, and the way they allow us to revisit the above empirical rules in molecular photophysics.

The Kasha rule

Non-Kasha rule behavior

Few cases of the violation of the Kasha rule exist, and a well-documented example was first reported in 1955 for azulene [38] and confirmed by more recent studies [24, 39]. The classical explanation is that the S_1 and S_2 states lie sufficiently far apart that fluorescence is observed mostly from S_2. Other examples concern the pyrenes [40, 41] and naphthalene [41, 42]. All these molecules are relatively small size polyatomics. As the number of degrees of freedom of the molecule increases and with it, the density of states, one expects the Kasha rule to be more strictly observed.

At the end of the 1990s, we reported on a striking violation of the Kasha rule in the extreme case of the C_{70} molecule trapped in neon matrices at low temperatures [43–46]. As can be seen from Fig. 5a, fluorescence of both S_1 (A_2') and S_2 (E_1') states is observed for excitation at energies above the latter, while exciting the S_1 state yields only its own fluorescence (Fig. 5b). The transition between S_1 (A_2') and the singlet A_1' ground state is orbitally forbidden, but it can gain some intensity via Herzberg–Teller coupling. On the other hand, S_2 (E_1') is dipole allowed to the ground state. Its fluorescence was attributed to the fact that it lies 165 cm^{-1} above the S_1 state, which is less than the smallest vibrational quantum of the molecule (~200 cm^{-1}) so that energy cannot be converted into vibrational energy of the molecule, thus creating a bottleneck to intramolecular non-radiative relaxation. This represents the largest molecule for which the Kasha rule is violated. By ultrafast fluorescence studies using a streak camera with 20 ps time resolution, it was found that S_2 predominantly decays to S_1 by non-radiative relaxation in about 0.5 ns [46].

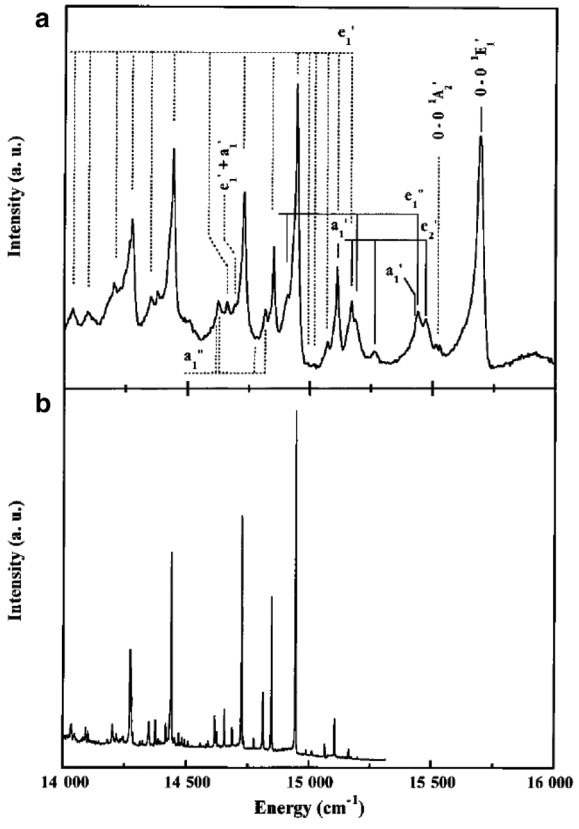

Fig. 5: Steady-state fluorescence spectrum of C_{70} in solid neon for excitation at (a) 470 nm (21 277 cm^{-1}) above the S_2 state, and (b) 644.16 nm (15 524 cm^{-1}) at the electronic origin of the S_1 ($^1A_2'$) state. Solid marks refer to the assignment of the $^1A_2'(S_1)$- $^1A_1'(S_0)$ transition, while dotted marks to those of the $^1E_1'(S_2)$- $^1A_1'(S_0)$ transition [43].

Our studies of the C_{60} in neon and argon matrices at low temperatures also showed steady-state emission from the three lowest singlet states, all of which are dipole-forbidden to the ground state, and are within 100 cm^{-1} from each other. Despite this small gap, which could be bridged by the activation of phonons in the rare gas lattice, the S_3 state was found to decay to the lower S_1/S_2 states, in 170 ps in Neon matrices and 70 ps in argon matrices.

In inorganic photophysics, there are a number of instances of non-Kasha behavior, for example, the (2-ferrocenyl)indene complex [47], or a Re(I)-bisthiazole complex [48]. In these cases, the violation of the Kasha rule has been associated to photoisomerization that leads to isomers with different emission characteristics. Another manifestation of non-Kasha behavior is the case of dual fluorescence between thermally equilibrated states in Ir(III) and Pt(II) complexes [49–53]. However, at room temperature the excited states are in thermal equilibrium and the "non-Kasha" behavior is masked by a single lifetime and a broad emission band. Temperature-dependent studies are then essential to identify the manifestation of non-Kasha behavior, as in the above case.

Intermediate cases

As already mentioned, with improvements of the fluorescence up-conversion method, it became possible to capture weak emission signals from higher lying states. Over the past few years, we documented a number of cases, especially among coordination chemistry complexes, where emission from higher lying electronic states was observed [54–56]. The cases of halogenated rhenium–carbonyl complexes [54], and more so of the osmium complex $Os(dmbp)_3$(dmbp = 4,4′-dimethyl-2,2′-biypridine) in ethanol [56] are examples where we detected intermediate 10–50 ps lived emissions. In the latter case, it was due to a higher triplet state lying at an energy ~2000 cm^{-1} above the lowest triplet state whose phosphorescence decays in 25 ns, due to a quantum yield of $\leq 5.0 \times 10^{-3}$.

The occurrence of such intermediate emissions imply that a weak proportion of population reaches the ground state bypassing the lowest electronic excited state. Although, they represent a violation of the Kasha–Vavilov rule, it is a mild one. Indeed, if we assume a typical pure radiative lifetime of microseconds for the triplet state, it corresponds to an emission quantum yield of 10^{-6} for such states, and they would indeed not be observable under steady-state detection conditions.

Relaxation at sub-vibrational time scales

At the other extreme is the observation of a fluorescence that mirrors the absorption band of the lowest excited state at the shortest time delays, i.e., within the pulse width of the pump laser, and regardless of the excitation energy. This is the case in Fig. 4 and it is better depicted in Fig. 6, which shows the absorption bands and the time-zero emission bands of $[Ru(bpy)_3]^{2+}$ and $[Fe(bpy)_3]^{2+}$ in solution. Similar observations were made on other Ru complexes [57] and were found to be independent of the solvent, symmetry of the complex and initially excited S_n state. The mirror profile of the emission implies that it occurs from a thermalized state, which seems paradoxical. The lowest singlet fluorescence in Ru- and Fe–polypyridine complexes is found to be very short-lived (<40 fs) [57]. In order to reach the S_1 state, the system has to relax the excess energy via electronic (internal conversion, IC) and vibrational levels (intramolecular vibrational redistribution, IVR). Taking its lifetime as an internal clock, this implies that the IVR/IC processes occur in <10 fs [57], i.e., on sub-vibrational time scales! It should however be stressed that thermalization is only with respect to the high frequency Franck-Condon modes that make up the modulations of the absorption band (Fig. 6). These modes dump their energy on a sub-vibrational time scale into the bath of low frequency, optically silent modes, in a fashion akin to a critically damped oscillator. When however, higher S_n states are excited, these very fast relaxation processes must take place in a strongly non-Born–Oppenheimer fashion for the IC to occur, probably involving conical intersections between excited state potential surfaces. These results also imply that IC/IVR within singlet states precedes ISC.

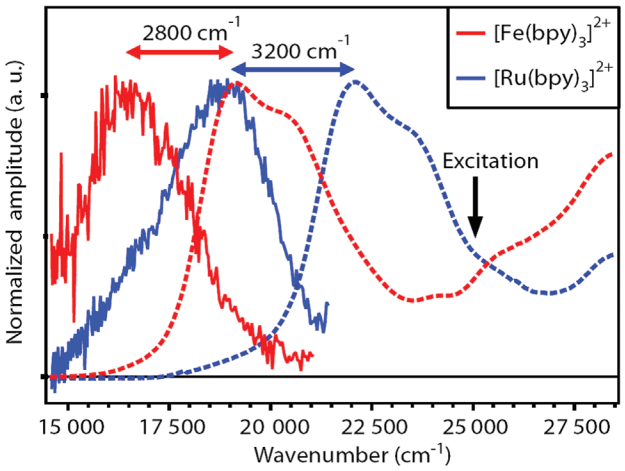

Fig. 6: Steady-state absorption spectra showing the ^{1}MLCT absorption band (dashed traces) and time-zero fluorescence spectra of $[Fe(bpy)_3]^{2+}$ and $[Ru(bpy)_3]^{2+}$ in water, excited at 25 000 cm^{-1} (black arrow). The horizontal arrows indicate the respective absorption-emission Stokes shift [33, 57, 58].

The idea of dumping the energy into low frequency, optically silent modes is difficult to verify in the above examples because the singlet lifetime is too short, but we verified it in the case of organic dyes, such as 2,5-diphenyloxazole (PPO) and para-terphenyl (pTP), pumped with a large excess of vibrational energy [36]. It was observed that at zero time delay, the mirror image of the fluorescence with respect to the lowest absorption band, is already present but it is structure-less. Thereafter, vibrational cooling of the low frequency modes and/or solvation dynamics occur on the time scale of several ps, leading to a structured fluorescence spectrum, identical to the steady-state spectrum.

In conclusion, the observation of a mirror image fluorescence to the absorption of the lowest singlet state at the shortest time delay does not imply ultrafast cooling, except for the high frequency Franck–Condon modes, because the excess energy is redistributed into low frequency ones.

Deviations from the heavy atom effect

Figure 4 nicely illustrates the ability of the broad band fluorescence detection with fs resolution to observe the change from fluorescence to phosphorescence. In this case ($[Ru(bpy)_3]^{2+}$) [33] and in the case of a whole series of Ru– and Fe–polypyridine complexes [57, 58], the decay of the ^{1}MLCT (<40 fs) fluorescence is reflected in the rise of the ^{3}MLCT state. Such ISC times are the shortest ever reported. Further investigations with various transition metal complexes showed completely erratic trends with respect to the value of the SOC of the metal atom, contrary to the expectations based on the above IUPAC definition of the heavy atom effect.

This is clear from Table 1, which shows the ISC times we measured for various Fe, Ru, Pt, Re, and Os complexes [33, 55–58, 62], in particularly: a) the ISC rate between the lowest singlet and triplet states of a diplatinum complex (Pt_2POP) was found to lie in the 10–30 ps range and to be solvent-dependent! [55]; b) In complexes such as $[Re(L)(CO)_3(bpy)]n^+$ (for L=Cl, Br, I, n=0; for L=Etpy=ethylpyridine, n=1), the ISC times (100–150 fs) are significantly longer than in the Fe or Ru complexes, but remarkably, they decreased in the sequence I–Br–Cl, in what appears as an inverse-heavy atom effect [54]. We also found a linear correlation between the ISC times and the Re-halogen stretch frequency for these complexes (Fig. 7), suggesting that structural changes mediate the spin transition.

The comparison between the Fe, Ru, Pt, Re, Ir and Os complexes also underlines the importance of the density of states. For example, $Os(dmbp)_3$ showed slower ISC times (Fig. 8) than $Os(bpy)_2(dpp)$, which

Table 1: Intersystem crossing times for the complexes investigated in Lausanne by fluorescence up-conversion and transient absorption spectroscopy, along with the spin-orbit constant of the metal atom.

Complex	ISC Transition	Time	Spin-orbit constant (eV)	References
$[Fe(bpy)_3]^{2+}$	^{1}MLCT-^{3}MLCT	<30 fs	0.05	[58]
$[Fe(bpy)_3]^{2+}$	^{3}MLCT-^{5}T	<130 fs		[59]
				[60]
$[Ru(bpy)_3]^{2+}$	^{1}MLCT-^{3}MLCT	≤30 fs	0.1	[33]
RuN719	^{1}MLCT-^{3}MLCT	≤30 fs		[57]
RuN3	^{1}MLCT-^{3}MLCT	≤45 fs		[57]
Dithione-dithiolato-Ni	^{1}MMLLCT-^{3}MMLLCT	6 ps	0.19	[61]
$[ReX(CO)_3bpy]^+$	^{1}MLLCT-^{3}MLLCT	85 fs	0.335	[54]
X = Cl				
= Br		130 fs		
= I		150 fs		
= etpy		130 fs		
$Os(dmbp)_3$	^{1}MLCT-^{3}MLCT	100 fs	0.37	[56]
$Os(bpy)_2(dpp)$	^{1}MLCT-^{3}MLCT	<50 fs		[56]
Pt_2POP	$^1A_{2U}$-$^3A_{2U}$	10–30 ps (solvent dep.)	0.583	[55]
Dithione-dithiolato-Pt/Pd	^{1}MMLLCT-^{3}MMLLCT	6 ps		[61]

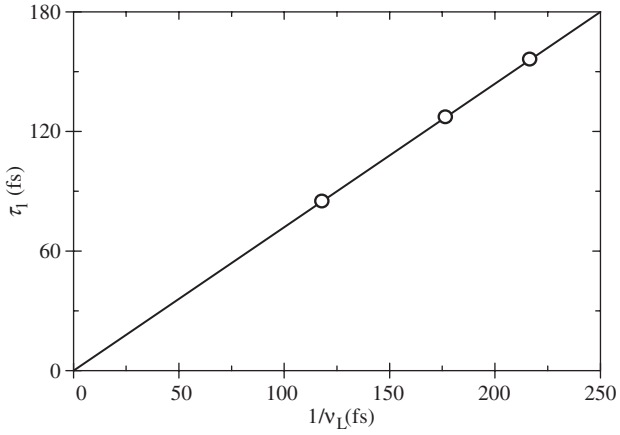

Fig. 7: Correlation of the ISC times measured in this work for the $[Re(L)(CO)_3(bpy)]$ (L=Cl, Br, I, from left to right) complexes with the vibrational period of the Re-L stretch mode in similar $[Re(L)(CO)_3(iPr\text{-}NdCHCHdN\text{-}iPr)]$ complexes, as derived from their resonance Raman spectra [63].

has a higher density of electronic and vibrational states as seen from its absorption spectrum [56] (dmbp is 4,4′-dimethyl-2,2′-biypridine, bpy is 2,2′-biypridine, and dpp is 2,3-dipyridyl pyrazine).

Thus, the IUPAC definition of the heavy atom effect needs to be revised. If a high spin-orbit coupling (SOC) constant is a necessary condition, it is not a sufficient one and other parameters, such as density of states, crossings of potential surfaces and structural rearrangements play an important role. In a way, it is like in electron transfer reactions: even if a large driving force is present, this does not mean an ultrafast electron transfer if the potential surfaces are weakly coupled or do not have the right crossings.

The rationale behind the observations reported in Table 1, and several ones from the literature, is the dynamical aspect of ISC rather than the steady-state one embodied in eq. 1. That is, the system explores regions of its configuration space and reaches the points in space where ISC is most favorable. The probablility of such events is, of course, enhanced when the density of states is higher. This is well described in ref. [64]

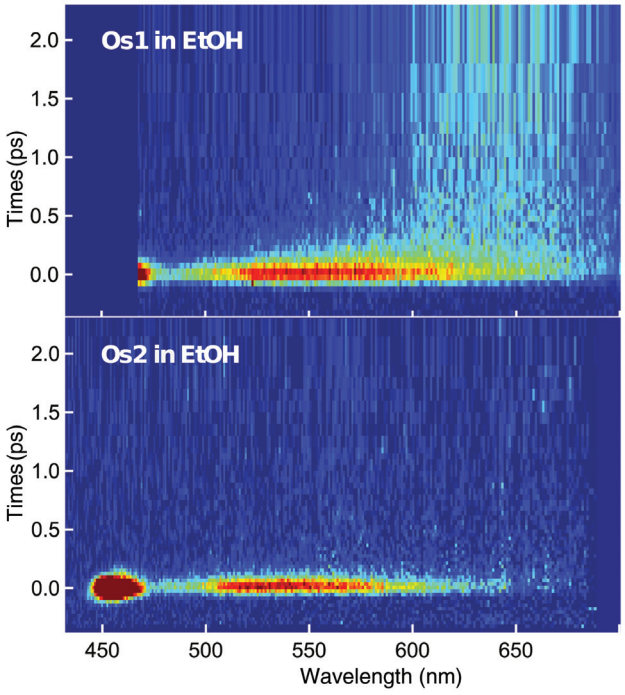

Fig. 8: Time-wavelength plots of the emission of Os(dmbp)3 (Os1) and Os(bpy)2(dpp) (Os2) (dmbp = 4,4′-dimethyl-2,2′-biypridine, bpy = 2,2′-biypridine, dpp = 2,3-dipyridyl pyrazine) in ethanol excited at 400 nm. The plots are normalized to the maximum of the fluorescence and the peak at 455 nm is the Raman line, which is cut on the blue by the detection window on the top panel.

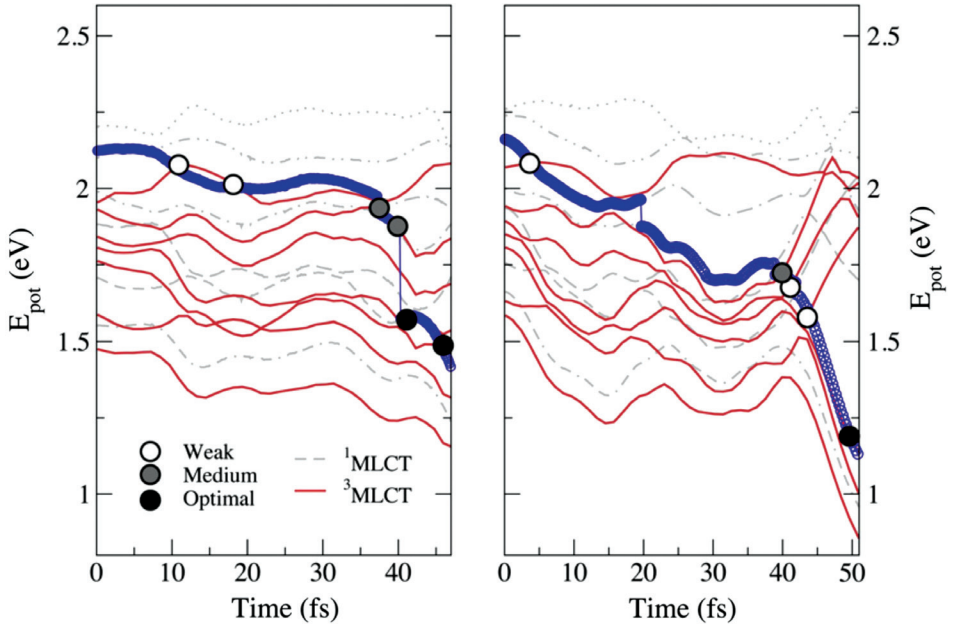

Fig. 9: Nonadiabatic molecular dynamics of $[Ru(bpy)_3]^{2+}$ in solution for the ISC from the ^{1}MLCT state to the ^{3}MLCT state. The two panels show the time series of the relevant excited state energies for the two trajectories discussed in the text. Singlet excited states (7 in total) are represented by gray dashed lines, triplet states (7 in total) by red continuous lines. The driving state is highlighted with blue circles. Analyzed crossings between singlet and triplet states (see ref. [64]) are represented by filled circles with the following color coding: white = weak, gray = medium, and black = optimal SOC strength. Reproduced from ref. [64].

and shown in Fig. 9. In this respect the above example with diplatinum complex shows that when the density of states is very low and crossings are unfavourable between states of different multiplicity, then the system develops a steady-state wave function, which then decays by ISC according to eq. 1.

The most remarkable ultrafast spin transition is in the case of Fe(II) spin cross-over complexes such as the above mentioned $Fe(bpy)_3$, which undergoes a $\Delta S = 2$ transition from the ^{1}MLCT state to the lowest lying excited state of quintet character, ^{5}T, in <150 fs (Table 1). We suspect that the origin of such ultrafast spin transition, which by the way also occur in Fe(II) porphyrin systems [65], may be mediated by an electron transfer between ligand and metal.

Ultrafast ISC also occurs in molecules containing light atoms, and there, the dynamical and energy degeneracy aspects of spin transitions are the key parameters, as was beautifully illustrated by Stolow and co-workers in recent ultrafast photoelectron studies on SO_2 [66] and cyclic α,β-Enones [67], in the gas phase. In the first case, they reported ISC from the mixed $^1B_1/^1A_2$ states to the $^3B_2$ state on time scales of 750 to 150 fs, depending on the excitation energy. These were rationalised by Gonzalez and co-workers [68] using ab initio molecular dynamics simulations. It was found that a strong elongation of the SO bonds and a small bending are pre-requisites for the ultrafast ISC. In the second case, it was found that upon singlet state excitation of 2-cyclopentenone an ISC occurs within 1.2 ps to the lowest triplet manifold, which was explained by a high SOC over an extended region of high singlet-triplet degeneracy explored by the system during its dynamics.

Conclusions

The increased sensitivity of detection schemes for steady-state fluorescence allows the unravelling of new cases where the Kasha Rule is violated and here we have presented the largest ever molecule that violates it in the case of the C_{70} molecule. The developments in ultrafast fluorescence spectroscopy also allow the detection of the emission from higher states with very low fluorescence yields. Finally, these new capabilities unravel new regimes of intramolecular dynamics (IC, ISC, IVR) in molecular systems. In particular: a) IVR from high frequency modes and IC can occur at sub-vibrational time scales; b) ultrafast ISC rates do not scale with the SOC of the "heavy-atom"; c) high ISC rates also occur in systems consisting of light atoms; d) ISC rates compete with IC rates in the regime of ultrafast dynamics; e) density of states and dynamical exploration of the configuration space are important parameters in ultrafast ISC events; f) the heavy-atom effect applies only in the steady-state regime, i.e., on time scales of ns or longer.

Acknowledgments: This work was supported by the Swiss NSF via the NCCR MUST.

References

[1] A. H. Zewail. *J. Phys. Chem. A.* **104**, 5660 (2000).
[2] J. Gardecki, M. L. Horng, A. Papazyan, M. Maroncelli. *J. Mol. Liq.* **65–66**, 49 (1995).
[3] M. Du, G. R. Fleming. *Biophys. Chem.* **48**, 101 (1993).
[4] M. H. Cho, S. J. Rosenthal, N. F. Scherer, L. D. Ziegler, G. R. Fleming. *J. Chem. Phys.* **96**, 5033 (1992).
[5] P. Hamm, M. T. Zanni. *Concepts and Methods of 2d Infrared Spectroscopy*, Cambridge University Pres, Cambridge, New York (2011).
[6] G. S. Schlau-Cohen, A. Ishizaki, G. R. Fleming. *Chem. Phys.* **386**, 1 (2011).
[7] A. Ghosh, R. M. Hochstrasser. *Chem. Phys.* **390**, 1 (2011).
[8] B. A. West, A. M. Moran. *J. Phys. Chem. Lett.* **3**, 2575 (2012).
[9] B. A. West, P. G. Giokas, B. P. Molesky, A. D. Ross, A. M. Moran. *Opt. Express* **21**, 2118 (2013).
[10] A. Cannizzo. *Phys. Chem. Chem. Phys.* **14**, 11205 (2012).
[11] A. Ajdarzadeh Oskouei, O. Bram, A. Cannizzo, F. van Mourik, A. Tortschanoff, M. Chergui. *J. Mol. Liq.* **141**, 118 (2008).
[12] A. Ajdarzadeh Oskouei, O. Braem, A. Cannizzo, F. van Mourik, A. Tortschanoff, M. Chergui. *Chem. Phys.* **350**, 104 (2008).
[13] A. Ajdarzadeh Oskouei, A. Tortschanoff, O. Bram, F. van Mourik, A. Cannizzo, M. Chergui. *J. Chem. Phys.* **133**, 064506 (2010).

[14] A. Ajdarzadeh, C. Consani, O. Bram, A. Tortschanoff, A. Cannizzo, M. Chergui. *Chem. Phys.* **422**, 47 (2013).
[15] S. D. Moran, A. M. Woys, L. E. Buchanan, E. Bixby, S. M. Decatur, M. T. Zanni. *P. Natl. Acad. Sci. USA* **109**, 3329 (2012).
[16] B. A. West, B. P. Molesky, P. G. Giokas, A. M. Moran. *Chem. Phys.* **423**, 92 (2013).
[17] G. Aubock, C. Consani, R. Monni, A. Cannizzo, F. van Mourik, M. Chergui. *Rev. Sci. Instrum.* **83**, 093105 (2012).
[18] G. Aubock, C. Consani, F. van Mourik, M. Chergui. *Opt. Lett.* **37**, 2337 (2012).
[19] C. Consani, G. Aubock, F. van Mourik, M. Chergui. *Science* **339**, 1586 (2013).
[20] M. Chergui. *Acta. Crystallogr. A* **66**, 229 (2010).
[21] L. X. Chen, X. Y. Zhang, J. V. Lockard, A. B. Stickrath, K. Attenkofer, G. Jennings, D. J. Liu. *Acta. Crystallogr. A* **66**, 240 (2010).
[22] J. R. Lakowicz. *Principles of Fluorescence Spectroscopy,* Springer, New York (2006).
[23] M. Kasha. *Discuss Faraday Soc.* **9**, 14 (1950).
[24] P.Klán, J. Wirz. *Photochemistry of Organic Compounds: From Concepts to Practice,* Wiley, Chichester, West Sussex, UK (2009).
[25] <http://goldbook.iupac.org/H02756.html>.
[26] R. Bakova, M. Chergui, C. Daniel, A. Vlcek, S. Zalis. *Coordin. Chem. Rev.* **255**, 975 (2011).
[27] A. D. Kirk, P. E. Hoggard, G. B. Porter, M. G. Rockley, M. W. Windsor. *Chem. Phys. Lett.* **37**, 199 (1976).
[28] G. Porter. *Proc. R Soc. Lon. Ser. A* **200**, 284 (1950).
[29] A. Mokhtari, J. Chesnoy, A. Laubereau. *Chem. Phys. Lett.* **155**, 593 (1989).
[30] S. Arzhantsev, M. Maroncelli. *Appl. Spectrosc.* **59**, 206 (2005).
[31] M. Sajadi, M. Weinberger, H. A. Wagenknecht, N. P. Ernsting. *Phys. Chem. Chem. Phys.* **13**, 17768 (2011).
[32] S. Haacke, R. A. Taylor, I. Bar-Joseph, M. J. S. P. Brasil, M. Hartig, B. Deveaud. *J. Opt. Soc. Am. B* **15**, 1410 (1998).
[33] A. Cannizzo, F. van Mourik, W. Gawelda, G. Zgrablic, C. Bressler, M. Chergui. *Angew. Chem. Int. Ed.* **45**, 3174 (2006).
[34] X. X. Zhang, C. Würth, L. Zhao, U. Resch-Genger, N. P. Ernsting, M. Sajadi. *Rev. Sci. Instrum.* **82**, 063108 (2011).
[35] G. Zgrablic, K. Voitchovsky, M. Kindermann, S. Haacke, M. Chergui. *Biophys. J.* **88**, 2779 (2005).
[36] A. Cannizzo, O. Bram, G. Zgrablic, A. Tortschanoff, A. A. Oskouei, F. van Mourik, M. Chergui. *Opt. Lett.* **32**, 3555 (2007).
[37] C. Bonati, A. Cannizzo, D. Tonti, A. Tortschanoff, F. van Mourik, M. Chergui. *Phys. Rev. B* **76**, 033304 (2007).
[38] M. Beer, H. C. Longuethiggins. *J. Chem. Phys.* **23**, 1390 (1955).
[39] B. D. Wagner, D. Tittelbachhelmrich, R. P. Steer. *J. Phys. Chem.* **96**, 7904 (1992).
[40] P. A. Geldof, R. P. H. Rettschnick, G. J. Hoytink. *Chem. Phys. Lett.* **4**, 59 (1969).
[41] P. Wannier, P. M. Rentzepis, J. Jortner. *Chem. Phys. Lett.* **10**, 193 (1971).
[42] T. Deinum, C. J. Werkhoven, J. Langelaar, R. P. Rettschnick, J. D. Vanvoors. *Chem. Phys. Lett.* **19**, 29 (1973).
[43] A. Sassara, G. Zerza, M. Chergui. *J. Phys. Chem. A* **102**, 3072 (1998).
[44] A. Sassara, G. Zerza, V. Ciulin, M. T. Portella-Oberli, J. D. Ganiere, B. Deveaud, M. Chergui. *J. Lumin.* **83–84**, 29 (1999).
[45] G. Zerza, A. Sassara, M. Chergui. *Synthetic. Met.* **103**, 2386 (1999).
[46] A. Sassara, G. Zerza, M. Chergui, V. Ciulin, J. D. Ganiere, B. Deveaud. *J. Chem. Phys.* **111**, 689 (1999).
[47] S. Scuppa, L. Orian, A. Donoli, S. Santi, M. Meneghetti. *J. Phys. Chem. A* **115**, 8344 (2011).
[48] K. E. Henry, R. G. Balasingham, A. R. Vortherms, J. A. Platts, J. F. Valliant, M. P. Coogan, J. Zubieta, R. P. Doyle. *Chem. Sci.* **4**, 2490 (2013).
[49] Y. S. Yeh, Y. M. Cheng, P. T. Chou, G. H. Lee, C. H. Yang, Y. Chi, C. F. Shu, C. H. Wang. *Chemphyschem* **7**, 2294 (2006).
[50] K. K. W. Lo, K. Y. Zhang, S. K. Leung, M. C. Tang. *Angew. Chem. Int. Ed.* **47**, 2213 (2008).
[51] D. N. Kozhevnikov, V. N. Kozhevnikov, M. Z. Shafikov, A. M. Prokhorov, D. W. Bruce, J. A. G. Williams. *Inorg. Chem.* **50**, 3804 (2011).
[52] S. Ladouceur, L. Donato, M. Romain, B. P. Mudraboyina, M. B. Johansen, J. A. Wisner, E. Zysman-Colman. *Dalton T.* **42**, 8838 (2013).
[53] S. Ladouceur, L. Donato, M. Romain, B. P. Mudraboyina, M. B. Johansen, J. A. Wisner, E. Zysman-Colman. *Dalton T.* **42**, 16974 (2013).
[54] A. Cannizzo, A. M. Blanco-Rodriguez, A. El Nahhas, J. Sebera, S. Zalis, A. Vlcek, M. Chergui. *J. Am. Chem. Soc.* **130**, 8967 (2008).
[55] R. M. van der Veen, A. Cannizzo, F. van Mourik, A. Vlcek, M. Chergui. *J. Am. Chem. Soc.* **133**, 305 (2011).
[56] O. Bram, F. Messina, E. Baranoff, A. Cannizzo, M. K. Nazeeruddin, M. Chergui. *J. Phys. Chem. C* **117**, 15958 (2013).
[57] O. Bram, F. Messina, A. M. El-Zohry, A. Cannizzo, M. Chergui. *Chem. Phys.* **393**, 51 (2012).
[58] W. Gawelda, A. Cannizzo, V. T. Pham, F. van Mourik, C. Bressler, M. Chergui. *J. Am. Chem. Soc.* **129**, 8199 (2007).
[59] C. Bressler, C. Milne, V. T. Pham, A. ElNahhas, R. M. van der Veen, W. Gawelda1, S. Johnson, P. Beaud, D. Grolimund, M. Kaiser, C. N. Borca, G. Ingold, R. Abela, M. Chergui. *Science* **323**, 489 (2009).
[60] C. Consani, M. Premont-Schwarz, A. ElNahhas, C. Bressler, F. van Mourik, A. Cannizzo, M. Chergui. *Angew. Chem. Int. Edit* **48**, 7184 (2009).
[61] F. Frei, A. Rondi, D. Espa, M. L. Mercuri, L. Pilia, A. Serpe, A. Odeh, F. Van Mourik, M. Chergui, T. Feurer, P. Deplano, A. Vlček, A. Cannizzo. *Dalton T.* **43**, 17666 (2014).
[62] M. Chergui. *Dalton T.* **41**, 13022 (2012).
[63] B. D. Rossenaar, D. J. Stufkens, A. Vlcek. *Inorg. Chem.* **35**, 2902 (1996).
[64] I. Tavernelli, B. F. E. Curchod, U. Rothlisberger. *Chem. Phys.* **391**, 101 (2011).

[65] J. L. Martin, M. H. Vos. *Annu. Rev. Bioph. Biom.* **21**, 199 (1992).
[66] I. Wilkinson, A. E. Boguslavskiy, J. Mikosch, J. B. Bertrand, H. J. Worner, D. M. Villeneuve, M. Spanner, S. Patchkovskii, A. Stolow. *J. Chem. Phys.* **140**, 204301 (2014).
[67] O. Schalk, M. S. Schuurman, G. R. Wu, P. Lang, M. Mucke, R. Feifel, A. Stolow. *J. Phys. Chem. A* **118**, 2279 (2014).
[68] S. Mai, P. Marquetand, L. Gonzalez. *J. Chem. Phys.* **140**, 204302 (2014).